

SYMBOLIC DYNAMICS IN MATHEMATICS, PHYSICS, AND ENGINEERING

NICHOLAS B. TUFILLARO

ABSTRACT. I discuss several applications of symbolic dynamics and topological analysis to problems in mathematics, physics, and engineering. These are notes based on a talk presented on September 26, 1997 at the Institute for Mathematics and its Applications (IMA <http://www.ima.umn.edu>) as part of their Industrial Problems Seminar. The IMA is located in the Mathematics Department at the University of Minnesota.

1. INTRODUCTION

The mathematical aspects of this talk cover several topics, including kneading theory, horseshoes, and braid analysis. I first look at standard examples from the nonlinear dynamics literature which I use to illustrate the rudiments of symbolic dynamics. Specifically, I start by examining the dynamics of the quadratic map (and other unimodal maps), and the Rossler system of differential equations. Next, I turn to some examples from physics which also illustrate unimodal behavior such as the motions of a vibrating string and chemical oscillations in the Belousov-Zhabotinskii reaction. After learning about symbolic dynamics from these examples I then finish by showing how to use a symbolic analysis in a typical engineering application where the goal is often to detect (and possibly control) bifurcations found in noisy experimental data. Specifically, I review a recent application from engineering where symbolic dynamics is used to model and diagnosis cycle variability in internal combustion engines.

The different emphasis of the applications in the different disciplines is summarized in Table 1. The recent applications in physics and engineering suggest that symbolic dynamics is emerging as a new and potentially powerful tool for nonlinear system identification and diagnosis.

The general strategy for using symbolic dynamics as an analysis and diagnostic tool is as follows:

Date: 6 January 1998.

Key words and phrases. symbolic dynamics, nonlinear dynamics, diagnostics.

Thanks to Warren Weckesser for preparing notes from the talk.

| Discipline | Method | Goals | Emphasis |
|--------------------|--|--|----------------------|
| Mathematics | Generating partition on phase space | faithful map, 1 - 1, $n - 1$ | <i>proving</i> |
| Physics | (approximate) generating partition, with experimental resolution | model system, state identification, verification | <i>understanding</i> |
| Engineering | map for data reduction, simple and robust | diagnose, distinguish | <i>doing</i> |

TABLE 1. Symbolic dynamics in mathematics, physics, and engineering. The germ of the ideas is the same in each discipline, but the goals and implementations can be very different.

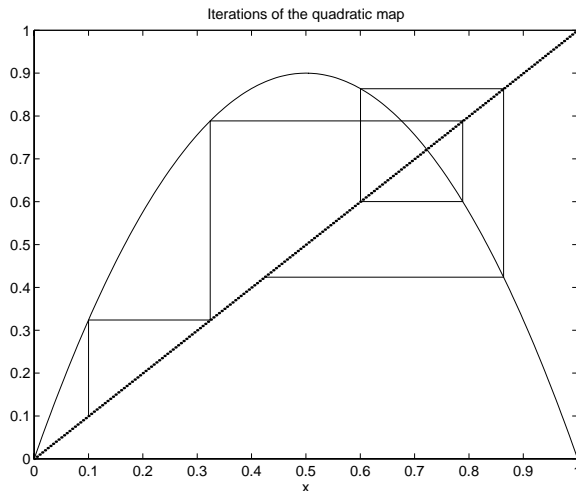


FIGURE 1. The quadratic map, with $\lambda = 3.5$. The vertical and horizontal lines show five iterates of the point $x_0 = 0.1$.

- Identify/specify the topological class/type.
- Set up a “symbol dynamics” for that particular class. (The *symbolic dynamics* are the *topological coordinates* appropriate for nonlinear problems.)
- Extract as much information as you can based on topology alone before considering metric properties. Identify/measure “topological parameters” if possible.

These ideas will be developed below.

Another point of this talk is to begin to understand some of the elements needed for effective collaborations between academia and industry. My experience as scientist and engineer leads me to believe that the different goals and problems that arise in academic research and industrial development are usually not properly understood or communicated in an afternoon. Rather, it really takes an immersion in each others’ work environment and culture to understand what the goals are, how things really work, and how to get things done. In my opinion, there is more than a difference in vocabulary stifling effective collaboration between workers in industry and academia.

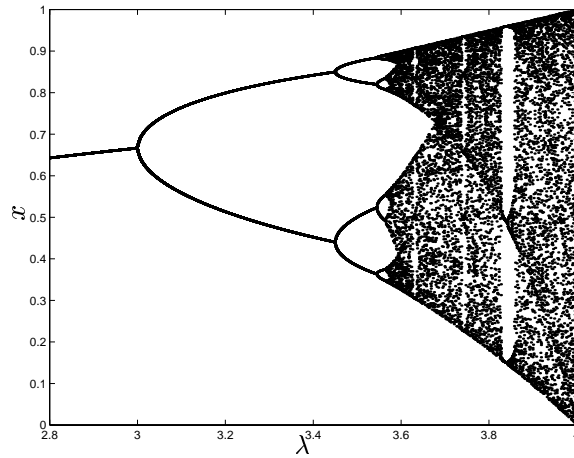
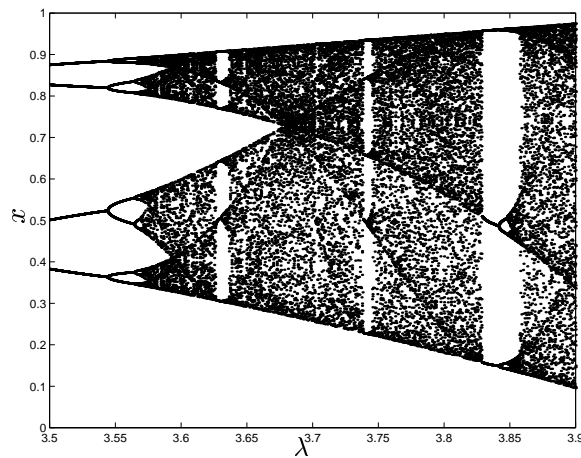
2. UNIMODAL MAPS AND KNEADING THEORY

The prototypical example of a unimodal map is the *quadratic map*:

$$(1) \quad x_{n+1} = \lambda x_n(1 - x_n).$$

Figure 1 shows $f(x) = \lambda x(1 - x)$, and includes a few iterations of the point $x_0 = 0.1$. In general, a *unimodal map* maps an interval I into itself, has a single critical point C in I , and is monotone increasing on the left of C and decreasing on the right. For the quadratic map, $I = [0, 1]$ and $C = 1/2$. The key topological property of a unimodal map is that it stretches and folds the interval I into itself.

One of the motivating reasons for studying the quadratic map is to understand the diagram shown in Figure 2. A closer view of part of this plot is shown in Figure 3. In each of these plots, a large sequence of increasing values of λ are generated. For each value of λ , we set $x_0 = 0.75$, and iterate the quadratic map 1000 times. We then plot the next 32 values in the iteration versus λ . These plots provide a rough picture of the asymptotic behavior of the quadratic map. For example, Figure 2 shows that for $\lambda < 3$, there is a stable equilibrium. (Indeed, it is easy to prove

FIGURE 2. Bifurcation diagram for the quadratic map, $2.8 < \lambda < 4$.FIGURE 3. A closer look at the bifurcation diagram for the quadratic map, $3.5 < \lambda < 3.9$.

that for $1 < \lambda < 4$, $x = \frac{\lambda-1}{\lambda}$ is an equilibrium, and it is stable for $1 < \lambda < 3$.) At $\lambda = 3$, the equilibrium becomes unstable, and a stable period 2 orbit is born. As λ is increased, the period 2 orbit eventually becomes unstable, and a period 4 orbit is born. This sequence of period doubling bifurcations appears to continue as λ is increased, but there is not sufficient resolution in the figures to see what happens. We can see a stable period 6 orbit at $\lambda \approx 3.63$, and a stable period 3 orbit at $\lambda \approx 3.83$.

In principle, we could determine all the periodic orbits (and determine their stability) by solving the appropriate formula. For example, period 3 orbits satisfy $x = f(f(f(x)))$. However, these equations quickly become intractable as the period increases. It has also been observed that very similar bifurcation diagrams can be found with other unimodal maps, suggesting that the qualitative structure of the bifurcation diagram is not unique to the quadratic map. The phenonema illustrated by the “universal” aspects of the bifurcation diagrams can be elucidated with symbolic dynamics and kneading theory.

To set up the *symbolic dynamics* of this system, we must first define a *partition*. Informally a partition is the separation of phase space into disjoint regions. By creating this partition we can go from a continuous description of a physical process to a discrete description composed of a finite (usually just a few) symbols. One of the first goals of symbolic dynamics is to understand the connection between continuous systems and discrete systems with (typically) a small alphabet.

For the quadratic map with $0 \leq \lambda \leq 4$, $I = [0, 1]$. We define $I_0 = [0, 1/2)$, $C = 1/2$, and $I_1 = (1/2, 1]$. Given x_0 , we define x_n by (1). We now define

$$s_n = \begin{cases} 0 & \text{if } x_n \in I_0, \\ C & \text{if } x_n = C, \\ 1 & \text{if } x_n \in I_1. \end{cases}$$

The *symbol sequence* or *itinerary* of the point x_0 is the sequence $S(x_0) = \{s_0, s_1, s_2, s_3, \dots\}$. For example, if $\lambda = 3.5$ and $x_0 = 0.1$ (see Figure 1), then $S(0.1) = \{0, 0, 1, 1, 1, 0, \dots\}$. The quadratic map acts on the sequence as a *shift*:

$$S(f^t(x)) = \sigma^t S(x) = \{s_t, s_{t+1}, s_{t+2}, \dots\},$$

where σ operates on sequences by discarding the left-most symbol, and shifting the rest of the sequence to the left.

I present a brief discussion of *kneading theory* [6, 7]. (A nice introduction to the theory is given by Devaney [8].) First, I define an ordering \prec on the itineraries which preserves the ordering on the interval. More precisely, if $S(x) \prec S(y)$, then $x < y$, and if $x < y$, then $S(x) \preceq S(y)$. Note that for a unimodal map, f is increasing on I_0 and decreasing on I_1 . After one iteration, the order of points in I_0 is maintained, while the order of points in I_1 is reversed. That is, if $x \in I_1$ and $y \in I_1$, and $x < y$, then $f(x) > f(y)$.

Define the order of the symbols to be $0 < C < 1$. Let's compare the symbol sequences $S(x) = \{s_0, s_1, s_2, \dots\}$ and $S(y) = \{t_0, t_1, t_2, \dots\}$. Clearly, if $s_0 < t_0$, then $x < y$, and if $s_0 > t_0$ then $x > y$. If $s_0 = t_0$, we compare s_1 and t_1 . However, we have to take into account that if $s_0 = t_0 = 1$, then the order of the points has been reversed by the first iteration of the mapping. Therefore, if $s_0 = t_0 = 1$ and $s_1 < t_1$, then it must be that $x > y$ (and $x < y$ if $s_1 > t_1$). Now suppose that the first two symbols agree, but, say, $s_2 < t_2$. If the first two symbols are 00, then there have been no reversals, so $x < y$. If the first two symbols are 01 or 10, then there has been one reversal, so $x > y$. Finally, if the first two symbols are 11, then there have been *two* reversals, so $x < y$.

In general, the order is determined by the order of the first pair of symbols that differ in the two sequences. In order to know the correct direction of the inequalities, we must keep track of how many times the order has been reversed. But this is just the number of 1s that appear in the segment of the sequences that agree, because a 1 means that the points are to the right of C , and their order will be reversed by the next iteration. If there are an *even* number of 1s, then we use the natural order of the first symbols that differ. If there are an *odd* number of ones, then the order of x and y is the reverse of the order of the first pair of different symbols.

These simple observations on the ordering of symbol sequences lead to some remarkable consequences. An illustration of the power of the kneading theory are the following theorems, which hold for a large class of unimodal maps. We define the *kneading sequence* $K(f)$ of the unimodal map f to be the itinerary of $x = f(C)$, i.e. $K(f) = S(f(C))$.

Theorem. Let \mathbf{s} be a symbol sequence. If $K(f)$ is not periodic, and $\sigma^i(\mathbf{s}) \prec K(f)$ for all $i \geq 0$, then there is a point $x \in I$ such that $S(x) = \mathbf{s}$.

This means we can construct an arbitrary symbol sequence \mathbf{s} , and if this sequence precedes the kneading sequence of the map, then there is a point in the interval with symbol sequence \mathbf{s} . A generalization is the following.

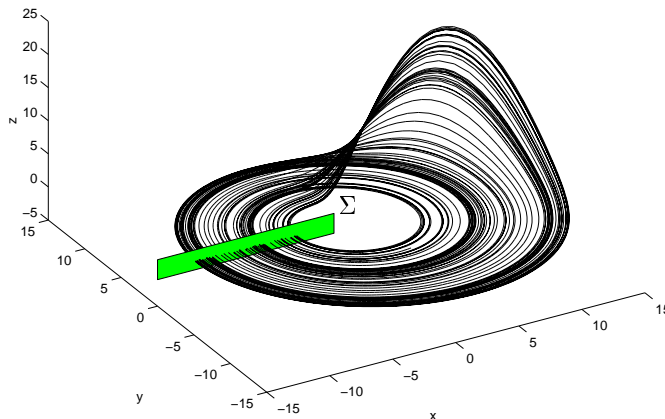


FIGURE 4. A single trajectory in the Rossler system.

Theorem. Suppose we are given two symbol sequences \mathbf{s} and \mathbf{t} , and there is a $y \in I$ such that $S(y) = \mathbf{t}$. If there is an $m \geq 0$ such that $\sigma^n(\mathbf{s}) \prec \sigma^m(\mathbf{t})$ for all $n \geq 0$, then there is $x \in I$ such that $S(x) = \mathbf{s}$.

These results prove especially useful when we consider periodic orbits. (See, for example, Chapter 1.19 of Devaney [8] for a more detailed introduction.) As we vary λ , the kneading sequence $K(f)$ changes, and the above results shows that the kneading sequence “determines” which periodic orbits exist. It turns out that for the quadratic map, the kneading sequence increases (in the sense of the order defined above) as λ increases. By combining the kneading theory with an additional property of the quadratic map (namely that it has a negative Schwarzian derivative), we obtain a detailed description of how periodic orbits arise as λ (and hence the kneading sequence) increases. This theory “explains” the qualitative features of the bifurcation diagram in Figure 2 which hold for all unimodal maps of the interval.

3. SYMBOLIC DYNAMICS AND ANALYSIS FOR CHAOTIC ATTRACTORS IN R^3

Now we turn from maps to flows to see how what we learned about unimodal maps can be applied to systems modeled by differential equations.

We consider three dimensional systems of differential equations that possess a chaotic attractor. As an example, we consider the Rossler equations:

$$(2) \quad \begin{aligned} \dot{x} &= -(y + z), \\ \dot{y} &= x + \alpha y, \\ \dot{z} &= \beta + (x - \mu)z. \end{aligned}$$

In this example, we use $\alpha = 0.17$, $\beta = 0.4$, and $\mu = 8.5$. A single (numerically computed) trajectory is shown in Figure 4. This trajectory provides a good approximation to the attractor.

Figure 5 shows (approximate) periodic orbits that were extracted from a single chaotic trajectory. Any two periodic orbits form a *knot*, and a collection of intertwined periodic orbits is called a *braid*. One key idea of *braid analysis* is to use the topological properties of a braid made up of a few periodic orbits to infer the existence of other periodic orbits. We saw that in the one dimensional maps, the

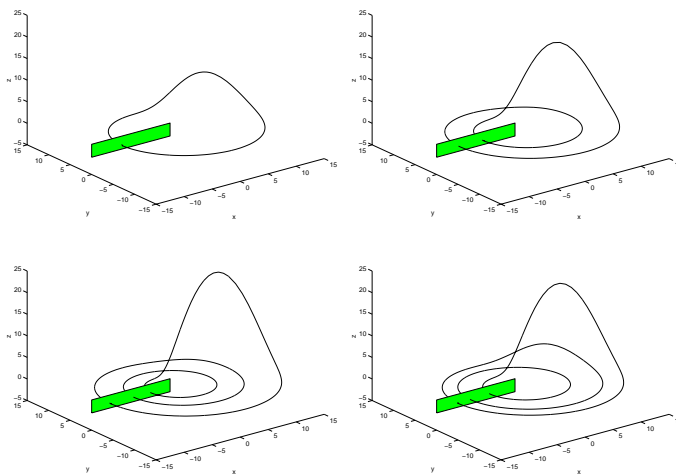


FIGURE 5. Some periodic orbits in the Rossler attractor.

existence of a given periodic orbit can imply the existence of others. There is an analogous result for two dimensional maps, which can be applied to a Poincaré section in a three dimensional flow.

One goal of this analysis is to identify an *organizing template*. A template is a branched manifold into which the periodic orbits can be placed in a way that preserves their topological structure in the flow. (See Tufillaro [5], Chapter 5, and the references therein.)

These ideas can be used to analyze experimental time series data. This type of analysis is often called *topological time series analysis*. The steps involved include identifying approximate periodic orbits in the data, embedding the data in R^3 (by using, for example, time-delay coordinates), and finding the topological relations among the periodic orbits. One may then be able to predict the organizing template of the experimental system.

One example of topological time series analysis is the work of Mindlin, et al [9], and Tufillaro [1], who have applied these methods to experimental data taken from the Belousov-Zhabotinskii reaction.

Another example is the analysis of the variations in the amplitude of a forced vibrating string. An elastic “string” (actually a metal wire) is stretched between two fixed points. The wire is subjected to a periodic force by running an alternating current through the wire and placing it in a magnetic field. When the string is forced near its fundamental frequency, the resulting vibrations have a fairly large amplitude. Some string models predict that the amplitude will vary chaotically in certain parameter ranges.

Molteno and Tufillaro [2] conducted experiments in which they observed a sequence of bifurcations and chaotic vibrations. O’Reilly and Holmes [3] have also observed chaotic vibrations. Tufillaro, et al [4] applied the methods of topological times series analysis to measurements of the transverse displacement of the wire at a single point. They extracted periodic orbits from the data, and they were able to identify an organizing template for the periodic orbits. In fact, they found that the dynamics could be described with a one dimensional unimodal map.

A similar result can be seen in the Rossler system. Figures 4, 6 and 7 show pictorially how the dynamics in the Rossler attractor can be reduced (at least approximately) to a one dimensional unimodal map. First, we consider a Poincaré cross section Σ , as shown in Figure 4. A plot of the crossings through Σ is given in Figure 6. The set of crossings appears to be one-dimensional. This leads us to consider the return map of just one variable, say x . In Figure 7, we plot $-x_{i+1}$ vs. $-x_i$,

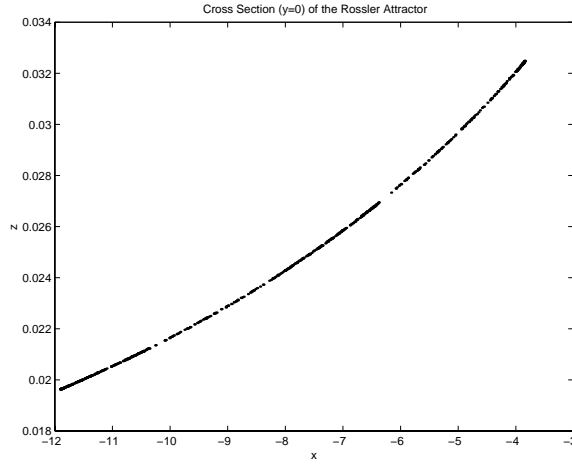


FIGURE 6. Cross section Σ of the Rossler attractor.

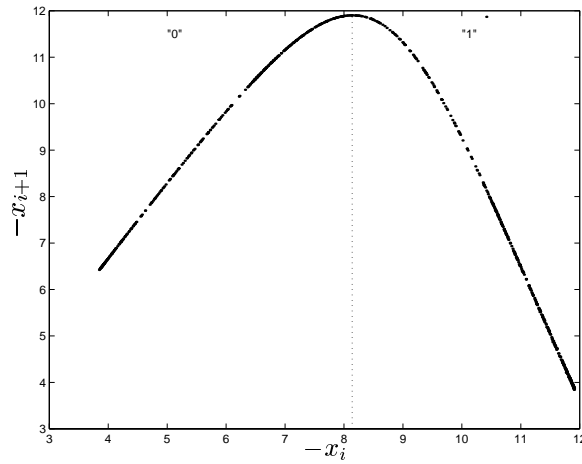


FIGURE 7. Plot of $-x_{i+1}$ vs. $-x_i$ for the cross section Σ of the Rossler attractor. This plots suggests that this map is well approximated by a one-dimensional unimodal map. The vertical dotted line indicates the location of the critical point of the map.

where the x_i are the x coordinates of the successive crossings of Σ . We see that this one dimensional map is unimodal, with a critical point at $x \approx -8.14$.

4. CYCLE VARIABILITY IN INTERNAL COMBUSTION ENGINES

Now that we have learned the rudiments of symbolic dynamics, we now point out how these ideas from mathematics and physics are used to motivated new methods that aid in the modeling and diagnosis of noisy nonlinear systems.

Recently, researchers at Oak Ridge National Labs and the University of Kentucky at Knoxville have applied the methods of symbolic time series analysis to the study of cycle variations in spark-ignited combustion engines [10, 11]. It has been observed for over 50 years that the combustion

efficiency of an internal combustion engine can vary significantly from one cycle to the next. This *cycle variability* is enhanced under lean (i.e. oxygen rich) fueling. The importance of understanding and controlling cycle variability has increased in recent years, as car manufacturers try to run their engines with leaner fuel mixtures to improve fuel efficiency and reduce NO_x emissions. The pressure for solving this problem comes from the new rules set forth by the Clean Air Act which will go into full effect at the beginning part of the next century.

In the four-stroke cycle, fuel and air enter the cylinder through the intake valve and the mixture is compressed when the piston moves up the cylinder. Near maximum compression, a spark ignites the mixture, and the resulting combustion forces the piston down the cylinder. This part of the cycle is used to perform work, such as driving the wheels of an automobile. When the piston again moves up the cylinder, the combustion by-products are forced out of the cylinder through the exhaust valve. Then, as the piston moves down the cylinder, fresh fuel and air enter the cylinder, and the cycle repeats.

One important cause of cycle variability is that, in a given cycle, combustion of the fuel may not be complete, and the unburned fuel may not be completely eliminated during the exhaust phase of the cycle. In this case, there will be extra fuel in the next cycle. This can result in significant variation in the power output of each cycle.

Daw, et al [10], have developed an empirical model of the combustion cycle. Their model maps the composition of the fuel-air mixture from one cycle to the next. Their analysis of this model reveals a sequence of period-doubling bifurcations as the *equivalence ratio* (ratio of fuel present relative to fuel required to consume all oxygen) of the injected fuel-air mixture is decreased from stoichiometry, in which there is just enough fuel to consume all the oxygen, towards the lean limit, in which there is excess oxygen. Two of their applications of symbolic encoding and dynamics will be discussed here. First, they used symbolic encoding to detect a bifurcation in noisy experimental data. Second, they used symbol sequence statistics as part of a model fitting procedure.

To explain these applications, we introduce the *symbol sequence histogram*. The first step in the analysis is to discretize the time series data into n discrete values. For example, in a binary partition ($n = 2$), data values are assigned the symbol “0” or “1” according to whether the data value is below or above a given threshold, respectively. (One approach for determining the appropriate threshold is ensure that in the resulting symbol sequence there is an equal number of each symbol.) Next, a symbol sequence vector length m is chosen, and the relative frequency of all possible symbol sequences of length m are calculated from the full symbol sequence. For example, if we have a binary partition and $m = 6$, we would calculate the relative frequency of the symbol sequences 000000, 000001, 000010, etc. that occur in the discretized data sequence. The symbol sequence length m is chosen so that the modified Shannon entropy

$$H = \frac{1}{\log n} \sum_i p_i \log p_i$$

is minimized. In this formula, p_i is the probability of the symbol sequence i , and n is the total number of *observed* sequences.

By expressing the length m symbol sequence as its decimal equivalent (e.g. $000000_2 = 0_{10}$, $000110_2 = 6_{10}$, $010101_2 = 21_{10}$, etc.), we can represent the symbol sequence statistics as a histogram, in which the horizontal axis is the decimal equivalent of the symbol sequence, and the vertical axis is the relative frequency of the symbol sequence.

For truly random data (and with a sufficiently large set of data), each symbol sequence of length m is equiprobable. Therefore, any significant deviation from equiprobability is evidence for deterministic structure in the data. For example, the existence of a stable period-2 solution would result in frequent occurrences of the symbol sequences 010101 and 101010, which would show up in the histogram as spikes at 21 and 42. (Indeed, in the absence of transients, noise, and measurement

error, the discretized data sequence would be ...01010101..., and *only* 21 and 42 would have non-zero probabilities.)

Detecting bifurcations in noisy experimental data. Finney, et al [11] conducted a series of experiments in which the equivalence ratio was varied from near stoichiometry to very lean, and the heat released in each cycle was determined for over 2800 cycles. By using a binary partition and a sequence length of six, they found evidence of a bifurcation from a steady solution to a period-2 solution near an equivalence ratio of 0.71. For larger equivalence ratios, the symbol sequence histograms show equiprobability for each symbol sequence. Near 0.71, the frequencies of 21 and 42 begin to show peaks, and these peaks increase significantly as the equivalence ratio is decreased.

Using symbol sequence statistics in model fitting. The empirical model of Daw, et al [10] includes several indeterminate parameters. To fit these parameters to the experimental data, the symbol sequence histogram was used as part of a model fitting procedure. The fit of the model was optimized by iteratively adjusting the parameters to give the best agreement between the symbol sequence histogram for iterations of the model and the experimental data. In their analysis, they found that higher level partitions were needed to accurately fit the model to the data. (A binary partition was sufficient to detect the period-2 bifurcation.) With this procedure, they were able to obtain a good match between the model and the experimental data, with physically plausible parameter values.

5. SUMMARY

The main point of this discussion is to illustrate how ideas originating in mathematics and physics for extracting *topological* information from a dynamical system and its associate nonlinear time series can be used to solve practical engineering problems by motivating new methods to diagnosis and model noisy nonlinear systems. Topological methods encoded by symbolic dynamics represent a new method of system and parameter identification which are relatively simple, robust, and degrade gracefully with noise. In a sense, they are the “proper” coordinates to extract “robust” information from (possibly noisy) nonlinear systems.

6. BIOGRAPHY OF NICHOLAS TUFILLARO

Nick Tuffillaro received his bachelor’s degree physics in 1982 at Reed College. He attended graduate school in physics at Bryn Mawr College, receiving the M.A. in 1987 and the Ph.D. in 1990. In the course of his career as a physicist and nonlinear dynamicist, he has spent a year as a Fulbright Scholar at the University of Otago in New Zealand, held an NSF/NATO Postdoctoral Fellowship at the University of Warwick, and spent a year at the Woods Hole Oceanographics Institute. He was also at the Center for Nonlinear Studies at Los Alamos National Labs for three years. He is currently at Hewlett-Packard Labs in Palo Alto, California. He is co-author of the book *An Experimental Approach to Nonlinear Dynamics and Chaos* [5], and numerous papers in physics and dynamical systems.

REFERENCES

1. N. B. Tuffillaro, Braid analysis of (low-dimensional) chaos, preprint.
2. T. C. A. Molteno and N. B. Tuffillaro, Torus doubling and chaotic string vibrations: experimental results, *Journal of Sound and Vibration* **137**, 327–330 (1990).
3. O. O’Reilly and P. J. Holmes, Non-linear, non-planar and non-periodic vibrations of a string, *Journal of Sound and Vibration* **153**, 413–435 (1992).
4. N. B. Tuffillaro, P. Wyckoff, R. Brown, T. Schreiber, and T. Molteno, Topological time series analysis of a string experiment and its synchronized model, *Physical Review E* **50** (6), 4509–4522 (1994).
5. N. B. Tuffillaro, T. A. Abbott, and J. P. Reilly, *An Experimental Approach to Nonlinear Dynamics and Chaos* (Addison-Wesley, 1992).

6. J. Milnor and W. Thurston, On iterated maps of the interval, *Lect. Notes in Math. 1342*, in *Dynamical Systems Proceedings*, University of Maryland 1986-87, J. C. Alexander, ed. (Springer-Verlag, Berlin, 1988).
7. J. Guckenheimer, Sensitive dependence to initial conditions for one-dimensional maps, *Comm. Math. Phys.* **70**, 133-160.
8. R. L. Devaney, *An Introduction to Chaotic Dynamical Systems* (Benjamin-Cummings, 1986).
9. G. B. Mindlin, H. G. Solari, M. A. Natiello, and X.-J. Hou, Topological analysis of chaotic time series data from the Belousov-Zhabotinskii reaction, *Journal of Nonlinear Science* **1**, 147-173 (1991).
10. C. S. Daw, C. E. A. Finney, M. B. Kennel, and F. T. Connolly, Cycle-by-cycle combustion variations in spark-ignited engines, *Proceedings of the Fourth Experimental Chaos Conference, Boca Raton, Florida USA, 1997 August 6-8*; C. S. Daw, M. B. Kennel, C. E. A. Finney, and F. T. Connolly, Observing and modeling nonlinear dynamics in an internal combustion engine, *Phys. Rev. E* **57** (3), 2811-2819 (1998).
11. C. E. A. Finney, J. B. Green, Jr. and C. S. Daw, Symbolic time-series analysis of engine combustion measurements, SAE International Congress and Exposition (Detroit, Michigan USA, 1998) (preprint); C. S. Daw, C. E. A. Finney, J. B. Green, Jr., M. B. Kennel, and J. F. Thomas, A simple model for cyclic variations in a spark-ignition engine, (SAE Paper No. 962086); C. Letellier, S. Meunier-Guttin-Cluzel, G. Gouesbet, F. Neveu, T. Duverger, and B. Cousyn, Use of the Nonlinear Dynamical System Theory to Study Cycle-to-Cycle Variations from Spark Ignition Engine Pressure Data (SAE Technical Paper Series 971640 — Reprinted from Diagnostics in SI and Diesel Engines SP-1279).

THE HEWLETT-PACKARD COMPANY, 1501 PAGE MILL ROAD MS-4AD, PALO ALTO CA 94304
E-mail address: nbt@hp1.hp.com